



**HAL**  
open science

## Variable flip angle T1 mapping and multi-echo T2 and T2\* mapping magnetic resonance imaging sequences allow quantitative assessment of canine lumbar disc degeneration

Nora Bouhsina, Léa Tur, Jean-baptiste Hardel, Stéphane Madec, Dominique Rouleau, Floriane Etienne, Jérôme Guicheux, Johann Clouet, Marion Fusellier

### ► To cite this version:

Nora Bouhsina, Léa Tur, Jean-baptiste Hardel, Stéphane Madec, Dominique Rouleau, et al.. Variable flip angle T1 mapping and multi-echo T2 and T2\* mapping magnetic resonance imaging sequences allow quantitative assessment of canine lumbar disc degeneration. *Veterinary Radiology and Ultrasound*, 2023, 64, pp.864 - 872. 10.1111/vru.13288 . hal-04599301

**HAL Id: hal-04599301**

**<https://hal.science/hal-04599301v1>**

Submitted on 3 Jun 2024



**HAL** is a multi-disciplinary open access archive for the deposit and dissemination of scientific research documents, whether they are published or not. The documents may come from teaching and research institutions in France or abroad, or from public or private research centers.

L'archive ouverte pluridisciplinaire **HAL**, est destinée au dépôt et à la diffusion de documents scientifiques de niveau recherche, publiés ou non, émanant des établissements d'enseignement et de recherche français ou étrangers, des laboratoires publics ou privés.



Distributed under a Creative Commons Attribution - NonCommercial - NoDerivatives 4.0 International License

# Variable flip angle T1 mapping and multi-echo T2 and T2\* mapping magnetic resonance imaging sequences allow quantitative assessment of canine lumbar disc degeneration

Nora Bouhsina<sup>1,2</sup>  | Léa Tur<sup>2</sup> | Jean-Baptiste Hardel<sup>2</sup> | Stéphane Madec<sup>1,2</sup> |  
Dominique Rouleau<sup>1,2</sup> | Floriane Etienne<sup>1,2</sup> | Jérôme Guicheux<sup>1</sup> | Johann Clouet<sup>1</sup> |  
Marion Fusellier<sup>1,2</sup> 

<sup>1</sup>Nantes Université, Oniris, CHU Nantes, INSERM, Regenerative Medicine and Skeleton, RMeS, Nantes, France

<sup>2</sup>Department of Diagnostic Imaging, CRIP, ONIRIS, College of Veterinary Medicine, Food Science and Engineering, Nantes, France

## Correspondence

Marion Fusellier, Nantes Université, Oniris, CHU Nantes, INSERM, Regenerative Medicine and Skeleton, RMeS, Nantes 44300, France.

Email: [marion.fusellier@oniris-nantes.fr](mailto:marion.fusellier@oniris-nantes.fr)

Nora Bouhsina and Léa Tur co-first authors.

## Abstract

Magnetic resonance imaging is the gold standard for diagnosing intervertebral disc (IVD) degeneration in dogs. However, published methods for quantifying severity or progression of IVD degeneration are currently limited. Mapping MRI sequences are used in humans for quantifying IVD degeneration but have rarely been applied in dogs. The objective of this prospective, method comparison study was to evaluate variable flip angle T1 mapping and multiecho T2 and T2\* mapping as methods for quantifying canine lumbar IVD degeneration in twenty canine patients without clinical signs of spinal disease. Ventral and dorsal lumbar IVD widths were measured on radiographs, and lumbar IVDs were assigned a qualitative Pfirrmann grade based on standard T2-weighted sequences. T1, T2, and T2\* relaxation times of the nucleus pulposus (NP) were measured on corresponding maps using manual-drawn ROIs. Strong intra- and interrater agreements were found ( $P < 0.01$ ) for NP relaxation times. Radiographic IVD widths and T1, T2, and T2\* mapping NP relaxation times were negatively correlated with Pfirrmann grading ( $P < 0.01$ ). Significant differences in T1 NP relaxation times were found between Pfirrmann grade I and the other grades ( $P < 0.01$ ). Significant differences in T2 and T2\* NP relaxation times were found between grade I and the other grades and between grades II and III ( $P < 0.01$ ). Findings indicated that T1, T2, and T2\* MRI mapping sequences are feasible in dogs. Measured NP relaxation times were repeatable and decreased when Pfirrmann grades increased. These methods may be useful for quantifying the effects of regenerative treatment interventions in future longitudinal studies.

## KEYWORDS

canine model, degeneration, intervertebral disc, quantitative MRI, relaxation time

**Abbreviations:** AF, annulus fibrosus; IVD, intervertebral disc; LBP, low back pain; NP, nucleus pulposus; PG, proteoglycan; ROI, region of interest.

This is an open access article under the terms of the [Creative Commons Attribution-NonCommercial-NoDerivs](https://creativecommons.org/licenses/by-nc-nd/4.0/) License, which permits use and distribution in any medium, provided the original work is properly cited, the use is non-commercial and no modifications or adaptations are made.

© 2023 The Authors. *Veterinary Radiology & Ultrasound* published by Wiley Periodicals LLC on behalf of American College of Veterinary Radiology.

## 1 | INTRODUCTION

Intervertebral disc (IVD) degeneration is a common affliction in dogs that can lead to IVD displacement and cause a broad variety of clinical signs, from cervical or back pain to severe neurological deficits.<sup>1</sup> IVD degeneration can occur spontaneously, with the natural aging of the IVD, or pathologically, consecutive to an early imbalance of the cellular and molecular interactions due to structural or mechanical failures.<sup>2</sup> In particular, changes in the molecular composition of the nucleus pulposus (NP) such as a decrease in the water and proteoglycan (PG) contents or degradation of the collagen fibers accompany the degenerative process.<sup>3</sup>

Veterinary practice has considerably increased the possibilities in diagnostic assessment by imaging of IVD degeneration in the past few years. Indeed, *in vivo* assessment of IVD degeneration by imaging is essential in the exploration of lumbar or lumbosacral pain. It is helpful in localizing the degenerated IVD, grading the severity of the findings, and tailoring the patient care. Although radiography can detect IVD width loss, calcification of the NP, and osseous changes of the vertebral endplates such as sclerosis and spondylosis,<sup>4</sup> this modality implies structural overlays and poor soft-tissue contrast due to the physical properties of X-rays. Similarly, although CT is increasingly available in veterinary medicine and overcomes the overlay issue of the vertebral reliefs identified with radiographs, subtle changes in the IVD can still not be assessed. Therefore, by its capacity to differentiate the soft tissues and especially the NP from the annulus fibrosus (AF), MRI has become the gold standard for the investigation of IVD degeneration.<sup>5</sup> Morphological assessment of the IVD is traditionally performed on conventional MRI sequences such as T2-weighted sequences. Initially described in human medicine,<sup>6,7</sup> Pfirrmann grading is one of the MRI grading systems available in veterinary medicine to qualitatively evaluate IVDs. It is the most widely used grading system to assess IVD degeneration, and it is the only system that has been validated in dogs.<sup>8</sup>

Mapping MRI, such as T1, T2, and T2\* mapping, has recently been developed to quantitatively assess the subtle and early degenerative changes that can be discerned in the IVD.<sup>9,10</sup> Measurement of the relaxation times of the NP and/or the AF can reflect the tissular alterations of the degenerated IVD. In particular, T2 mapping values, notably in humans, correlate with the water and the proteoglycan content of the tissue as well as with the Pfirrmann grading.<sup>11,12</sup> Moreover, human patients with chronic low back pain (LBP) exhibit a lower T2 relaxation time of the dorsal AF compared with asymptomatic patients.<sup>13</sup> T2 mapping has been studied in various animal models but, in the canine model, only one experimental study to date has assessed canine IVD degeneration using T2 mapping after induction of IVD degeneration in NC dogs.<sup>14</sup> As for humans and sheep, the T2 relaxation time decreased with IVD degeneration.<sup>14,15</sup> In parallel, one study established the T2 relaxation times for healthy NP in twelve beagles.<sup>16</sup> On the other hand, T2\* mapping evaluates the mobility of the water molecules and the spatial architecture of the macromolecules in the IVD.<sup>10,17</sup> In humans, it has been correlated with the Pfirrmann grade

and the glycosaminoglycan content of the NP.<sup>18,19</sup> Similarly, T1 mapping correlates with the water content<sup>20</sup> and decreases with IVD degeneration as assessed by the morphological Thompson grading.<sup>21</sup> Based on our review of the literature, T2\* and T1 mapping have not yet been applied to assess canine IVD degeneration.

In this context, the objective of this study was to quantitatively assess IVD degeneration in dogs using multiecho T2 and T2\* mapping and variable flip angle T1 mapping. It was hypothesized that MRI T1, T2, and T2\* relaxation times of the NP would correlate with canine IVD degeneration as assessed by Pfirrmann grading as well as the ventral and dorsal IVD widths on X-rays.

## 2 | MATERIALS AND METHODS

### 2.1 | Selection of subjects

The study was a prospective, methods comparison design. All procedures of this prospective study were approved by the Ethics Committee of the Veterinary School of Nantes ONIRIS (CERVO-2020-16-V). Initial inclusion criteria were adult dogs (>2 years of age) presenting at the ONIRIS referral center for MRI examination due to reasons other than spinal disease between September and November of 2020. Dogs were excluded if they had a history of lumbar or lumbosacral pain or were not stable enough to withstand long anesthesia. These decisions were based on clinical examinations carried out by the referring veterinarian or by the neurologist of our center.

### 2.2 | Data recording and analysis

After obtaining the owner's consent for inclusion in the study, each dog was anesthetized for the imaging procedures. The anesthesia was maintained by inhalation of isoflurane (1%–3%) after intravenous injection of premedication and induction protocols tailored to each patient's specificities.

Ventro-dorsal and lateral radiographs of the lumbar spine of each patient were performed (Convix 80 generator®, Universix 120® table, Picker) except if the patient already had radiographs of the spine within the month preceding the MRI exam. The exposure (mAs) and penetration power (kVp) values were adapted according to the size of the patient. Radiographs were read by a radiologist with 20 years of experience in diagnostic imaging. Dogs with radiographic diagnoses of major modifications in vertebral shape, length, height, and opacity were excluded.

After the initial referral MR scan was completed, MR images of the spine from T13 to S1 were obtained with a 1.5T MR scanner (Magnetom-Essenza®, Siemens Medical Solutions). The coil used for the sequences was adapted to the body form and weight of the patient. Sagittal T2-weighted images fast SE were acquired, followed by multiecho T2 and T2\* mapping and variable flip angle T1 mapping sequences (Table 1).

**TABLE 1** MRI technical parameters used for sampled dogs.

	Small and median sized dogs (<25 kg)				Large dogs (>25 kg)			
	T2-weighted Fast SE	T1 mapping	T2 mapping	T2* mapping	T2-weighted Fast SE	T1 mapping	T2 mapping	T2* mapping
Repetition time (ms)	3000	15	1300	428	3000	15	1300	428
Echo time (ms)	95	1.7	13.8/27.6/41.4/55.2/69	4.35/11.83/19.31/26.79/34.27	86	1.7	13.8/27.6/41.4/55.2/69	4.35/11.83/19.31/26.79/34.27
Flip angle (°)	120	5/26	180	69	120	5/26	180	69
Matrix	450 × 450	520 × 520	260 × 260	260 × 260	512 × 512	618 × 520	292 × 260	284 × 260
Section thickness (mm)	3	3	3	3	3	3	3	3
Slice interval (mm)	0.3	0.3	0.15	0.15	0.3	0.3	0.15	0.15
Pixel size (mm × mm)	0.6 × 0.6	0.5 × 0.5	1 × 1	1 × 1	0.6 × 0.6	0.5 × 0.5	1 × 1	1 × 1
Time of acquisition	3 min 29 s	2 min 53 s	5 min 03 s	1 min 40 s	3 min 59 s	3 min 23 s	5 min 38 s	1 min 49 s

Image analyses were performed by two observers, using an image analysis workstation (Horos<sup>®</sup> software, 3.0, Horos Project, Geneva, Switzerland; Apple Mac Mini<sup>®</sup> and Barco Eonis MDRC-2321<sup>®</sup> LED screen). The first observer had less than 1 year of experience in diagnostic imaging, while the second observer has 20 years of experience in diagnostic imaging. The ventral and dorsal IVD widths were measured on lateral radiographs. Based on the T2-weighted mid-sagittal images, a Pfirrmann score was assigned to each lumbar IVD.<sup>6,8</sup> To assess the relaxation times of the NP, a manual region of interest (ROI) was drawn around the NP using the “closed polygon” function (Figure 1) on the T2-weighted mid-sagittal image and then copied and pasted on the T1, T2, and T2\* mid-sagittal mapping images. For each IVD of each patient, the area of the ROI and the mean T1, T2, and T2\* relaxation times of this ROI were determined. The Pfirrmann grade, the ROI area, and the T1, T2, and T2\* relaxation times of the NP were determined independently for each IVD by the two observers who reached a consensus on the image analysis protocol. The first observer repeated these measurements twice to evaluate the intra-rater reliability with a minimum of one week between measurements to blind himself to his previous results.

### 2.3 | Statistics

The statistical analyses were performed by a statistician and a veterinary student (GraphPad Prism<sup>®</sup> software, 9.0.2, GraphPad Software). Intrarater reliability was assessed using Spearman's correlation for the Pfirrmann grade and Pearson's correlation for each relaxation time. The inter-rater reliability for the Pfirrmann grading was assessed using the weighted kappa coefficient. For the first observer, the grade that was assigned the most between the three readings was retained for the determination of the interrater reliability. Interrater reliabilities for the T1, T2, and T2\* relaxation times were determined using Pearson's correlation. Correlations between the relaxation times and the Pfirrmann grades and between the disc widths and the Pfirrmann grades were assessed using Spearman's and Pearson's correlations, respectively. They were considered significant when the *P*-value was <0.05. Significant differences between the Pfirrmann grades for each imaging parameter were evaluated using a Wilcoxon–Mann–Whitney test for the T1, T2, and T2\* relaxation times. Differences were considered to be statistically significant when the *P*-value was <0.05.

### 3 | RESULTS

Twenty dogs (7 female and 13 male) were included in this study, representing 120 IVD. The mean age was 86 months (30–139 months) and the mean weight was 17.7 kg (5–33.2 kg). Ten of the dogs were chondrodystrophic breeds (2 Pugs, 1 Beagle, 2 Cavalier King Charles Spaniels, 1 Boston Terrier, 3 French Bulldogs, and 1 Coton de Tulear). A power analysis and sample size estimation were performed before and after the data were collected with an alpha of 0.05 and power

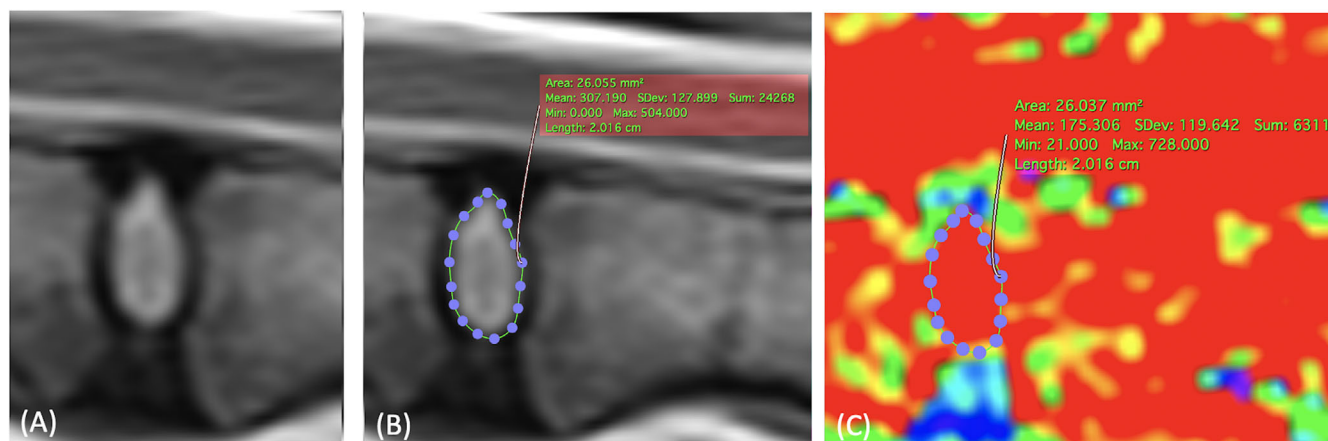


**FIGURE 1** The region-of-interest (ROI) drawing method used to delimitate the nucleus pulposus (NP) of canine lumbar intervertebral disc (IVD) on mid-sagittal T2-weighted MRI sequences (1.5 Tesla, 3 mm slice thickness, 0.3 mm slice interval, TE 86 ms, TR 3000 ms, flip angle 120°, 512 × 512 matrix). A, Healthy IVD graded Pfirrmann I, B, a manual ROI was drawn around the NP using the “closed polygon” function on the T2-weighted sagittal image, and then copied and pasted on the corresponding mapping images, including (C) T2 mapping images. [Color figure can be viewed at [wileyonlinelibrary.com](http://wileyonlinelibrary.com)]

**TABLE 2** Mean values and standard deviations of radiographic dorsal and ventral intervertebral disc widths and T1, T2, and T2\* mapping nucleus pulposus relaxation times for Pfirrmann grade.

Pfirrmann grading	Dorsal IVD widths (mm)		Ventral IVD widths (mm)		T1 mapping values (ms)		T2 mapping values (ms)		T2* mapping values (ms)	
	Mean	SD	Mean	SD	Mean	SD	Mean	SD	Mean	SD
I (n = 58)	3.965	0.895	5.187	1.312	1364	261.5	249.1	107.2	40.07	20
II (n = 25)	3.269	0.762	4.373	1.051	933.5	204.2	59.61	23.52	21.32	4.48
III (n = 33)	2.954	0.745	3.957	0.877	840.2	122.4	50.24	19.78	18.39	3.75
IV (n = 4)	3.621	0.513	4.429	0.721	762.2	68.77	74.37	68.56	18.78	8.29

Abbreviations: IVD, intervertebral disc; n, number; SD, standard deviation.

of 0.9 (clinical.com®). With our results of T1, T2, and T2\*, it required respectively 16, 14, and 46 IVD to highlight a difference between two Pfirrmann grades.

Intrarater analysis revealed strong agreement between the three different measures for all of the parameters ( $P < 0.001$ ,  $r > 0.91$ ). Given these results, the mean score of the three measures was used for interrater analysis. The interrater reliability for the Pfirrmann grade was almost perfect, with a Kappa coefficient of 0.885 (SE = 0.036; 95% CI = 0.813–0.956). The interrater agreement was also strong for the area of the ROI ( $\rho = 0.9077$ ;  $P < 0.001$ ), for T1 values ( $\rho = 0.9344$ ;  $P < 0.001$ ), T2 values ( $\rho = 0.9368$ ;  $P < 0.001$ ) and T2\* values ( $\rho = 0.8152$ ;  $P < 0.001$ ). For each MRI parameter, the mean value of the four measurements was retained to establish the correlation with the Pfirrmann grades.

There were 58/120 IVD (48%) that were classified as Pfirrmann grade I, 25/120 IVD (21%) were classified as grade II, 33/120 (28%) were classified as grade III, and 4/120 (3%) were classified as grade IV. None were classified as grade V. Complete agreement between the two observers was reached for 111/120 IVD (92.5%). Disagreement was

found for nine IVD, with only a difference of one grade, mostly between grades II and III (8/9).

The mean ventral and dorsal IVD widths assessed on radiographs and the mean MRI T1, T2, and T2\* relaxation times for each Pfirrmann grade are presented in Table 2. Overall, the additional scan time for the three mapping sequences compared with conventional spinal MR exam was less than 10 min. The mean ventral and dorsal IVD widths decreased significantly when the Pfirrmann grade increased ( $P < 0.0001$ ; Figure 2). Statistically significant differences were found between grades I and II ( $P = 0.0047$  for ventral condition and  $P = 0.0015$  for dorsal condition) and between grades I and III ( $P < 0.0001$  for both conditions). The mean T1 relaxation times decreased significantly when the Pfirrmann grade increased ( $P < 0.0001$ ; Figures 3 and 4). Statistically significant differences were found only between grades I and all the other grades ( $P < 0.0001$ ). The mean T2 relaxation times decreased significantly when the Pfirrmann grade increased ( $P < 0.0001$ ; Figure 5). Statistically significant differences were found between grade I and all the other grades ( $P < 0.0001$ ) and between grades II and III ( $P = 0.0347$ ). The mean T2\* relaxation

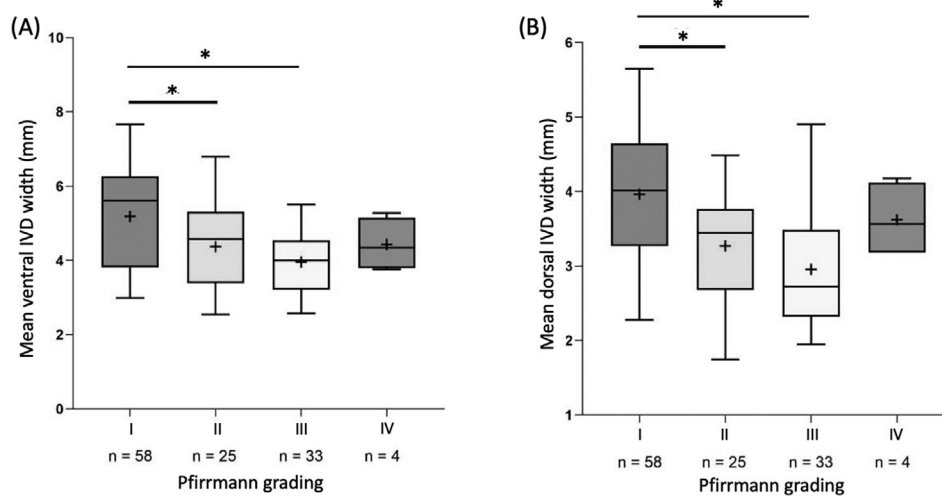


**FIGURE 2** Mean ventral (A) and dorsal (B) lumbar canine intervertebral disc (IVD) widths according to the Pfirrmann grading. For each dog, lumbar ventral and dorsal IVD widths were measured on the lateral radiographs. A negative correlation was found between disc widths and the Pfirrmann grades ( $P < 0.0001$ ). Significant differences were found between grades I and II and between grades I and III ( $*P < 0.001$ ).

times decreased significantly when the Pfirrmann grade increased ( $P < 0.0001$ ; Figure 6). Statistically significant differences were found between grade I and all the other grades ( $P < 0.01$ ) and between grades II and III ( $P = 0.0039$ ).

## 4 | DISCUSSION

Findings supported our hypotheses in that mean T1, T2, and T2\* mapping NP relaxation times had a strong intra- and interrater agreement and were correlated with radiographic IVD widths and T2 pulse sequence Pfirrmann grades. The additional mapping sequences took less than 10 min to perform. Our method allowed margins between the NP and the AF to be distinguished, which can be challenging in an advanced degenerated IVD. To overcome this difficulty, the contrast on the T2-weighted mid-sagittal image was systematically adapted to highlight the distinction between the two structures. Strong intra- and interagreements were found for the parameter "ROI area" using a manual "closed polygon" ROI drawing method even though the NP edges could be difficult to determine. Although the two observers did not have the same level of skill in diagnostic imaging, the interrater reliability was very high for all MR parameters. This implies that even operators without much experience in MRI should be able to reliably assess IVD degeneration using our drawing method on mapping sequences in dogs.

T1, T2, and T2\* relaxation times decreased when the qualitative Pfirrmann grade increased in our sample of dogs. Evaluation of the changes that occur in the lumbar human IVD by T2 and T2\* mapping have been well described, and numerous studies have investigated the correlation between T2 and T2\* times with various parameters used to characterize IVD degeneration. Most of these studies have correlated T2 or T2\* times in the IVD with the Pfirrmann grading system<sup>10,17,18,22-26</sup> and have demonstrated that there is a strong neg-

ative correlation between MR relaxation times and the MR qualitative scoring of the IVD degeneration, which is consistent with our findings. Only T2 mapping has been correlated with IVD degeneration in dogs.<sup>14</sup> This is the first published study describing T1 and T2\* mapping values and correlating them with IVD degeneration in a canine model. T1 mapping has rarely been used to assess IVD in humans as well as in animal models.<sup>25,27-29</sup> All of the studies to date have used the inversion recovery method to obtain T1 mapping sequences. This is also the first published study describing the application of the variable flip angle method to obtain T1 relaxation times in the canine NP.

Although MR mapping can enhance the evaluation by quantifying the degenerative changes that occur in canine IVD, its objective is not to replace the Pfirrmann grading. These two methods are complementary in the assessment of IVD degeneration. Nevertheless, only asymptomatic dogs were included in this study and, consequently, very few IVD were severely degenerated (4/120 were Pfirrmann grade IV and 0/120 were grade V). Moreover, no dogs with vertebral malformation or spondylosis were studied as it was a criterion of exclusion though these abnormalities can be a common feature in dogs suffering from back pain. A larger investigation with a higher number of IVD, a better repartition between the five grades of the Pfirrmann classification and which includes dogs with vertebral malformations or spondylosis may be of interest to assess the relevance of the mapping sequences on more severe grades of IVD degeneration. As MR mapping is relevant in the assessment of mildly degenerated canine IVD, the assumption can be made it should also be relevant for severely degenerated IVD but would be of limited interest given the fact that they would be easily detected on conventional MR images.

Numerous studies have reported correlations between relaxation times and the molecular composition of the NP. In particular, T2 and T2\* mapping reflects the hydration of the NP according to PG content,<sup>10-12,19,23,30</sup> which decreases with IVD degeneration. Finally, T1 relaxation times decrease with the water content.<sup>20</sup> Combining the



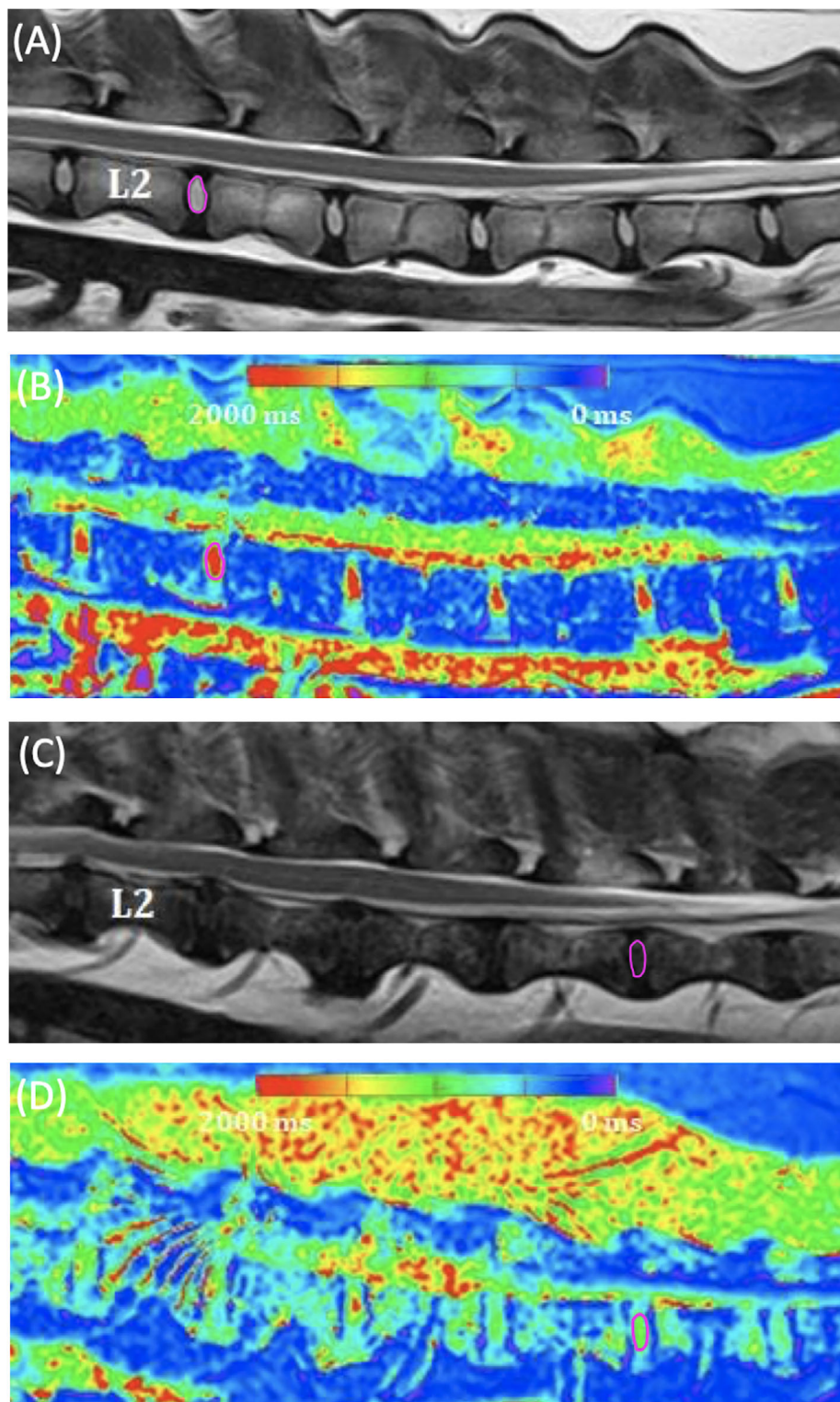


**FIGURE 3** Mid-sagittal T2-weighted images and the corresponding T1 maps of lumbar canine intervertebral discs (IVD) with different Pfirrmann grades. A, T2-weighted mid-sagittal image of a 4-year-old Golden Retriever with Pfirrmann grade I IVDs (1.5 Tesla, 3 mm slice thickness, 0.3 mm slice interval, TE 86 ms, TR 3000 ms, flip angle  $120^\circ$ ,  $512 \times 512$  matrix), and B, its corresponding T1 map (1.5 Tesla, 3 mm slice thickness, 0.3 mm slice interval, TE 1.7 ms, TR 14 ms, flip angles  $5^\circ/26^\circ$ ,  $618 \times 520$  matrix). The NP is visible (in red) with a high T1 relaxation time value. C, T2-weighted mid-sagittal image of an 11-year-old Beagle which IVDs classified as Pfirrmann grades III and IV (1.5 Tesla, 3 mm slice thickness, 0.3 mm slice interval, TE 95 ms, TR 3000 ms, flip angle  $120^\circ$ ,  $450 \times 450$  matrix), and D, the corresponding T1 map (1.5 Tesla, 3 mm slice thickness, 0.3 mm slice interval, TE 1.7 ms, TR 15 ms, flip angle  $5^\circ/26^\circ$ ,  $520 \times 520$  matrix). The NP is difficult to visualize and has a very low T1 relaxation value. Examples of manually designed regions of interest (ROI) have been drawn on T2-W images and pasted on corresponding T1 maps (purple polygons). [Color figure can be viewed at [wileyonlinelibrary.com](http://wileyonlinelibrary.com)]

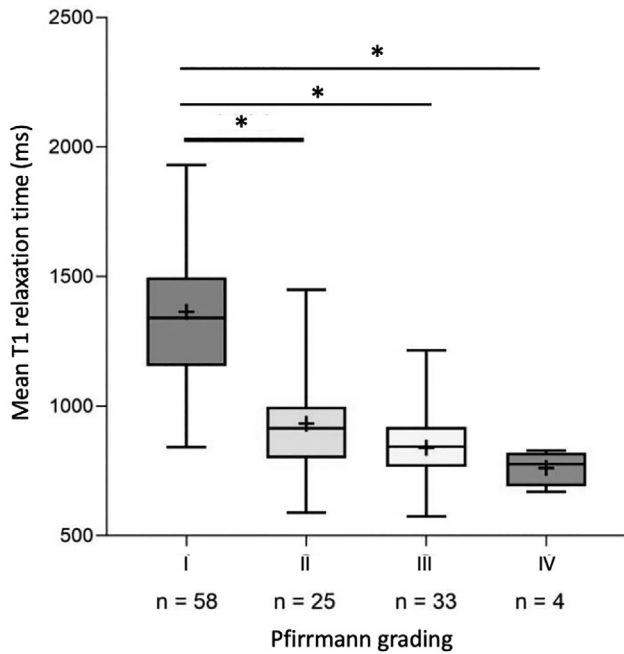


**FIGURE 4** Mean T1 relaxation time in the nucleus pulposus (NP) of the lumbar canine intervertebral discs (IVD) according to the Pfirrmann grading. The mean T1 relaxation time of the NP was measured by manually drawing a region of interest (ROI) around the NP of each lumbar canine IVD on the sagittal T2-weighted image and by copying it onto the T1 mapping image. A negative correlation was found between the T1 relaxation times and the Pfirrmann grades ( $P < 0.0001$ ). Significant differences were found between grade I and the other grades ( $*P < 0.05$ ).

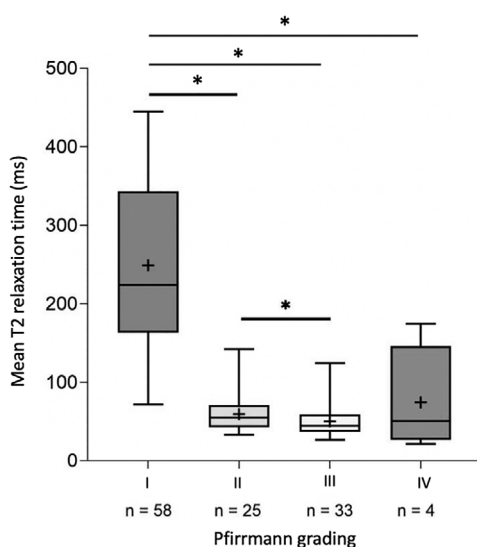


**FIGURE 5** Mean T2 relaxation time in the nucleus pulposus (NP) of the lumbar canine intervertebral discs (IVD) according to the Pfirrmann grading. The mean T2 relaxation time of the NP was measured by manually drawing a region of interest (ROI) around the NP of each lumbar canine IVD on the sagittal T2-weighted image and by copying it onto the T2 mapping image. A negative correlation was found between the T2 relaxation times and the Pfirrmann grades ( $P < 0.0001$ ). Significant differences were found between grade I and the other grades and between grades II and III ( $*P < 0.05$ ).

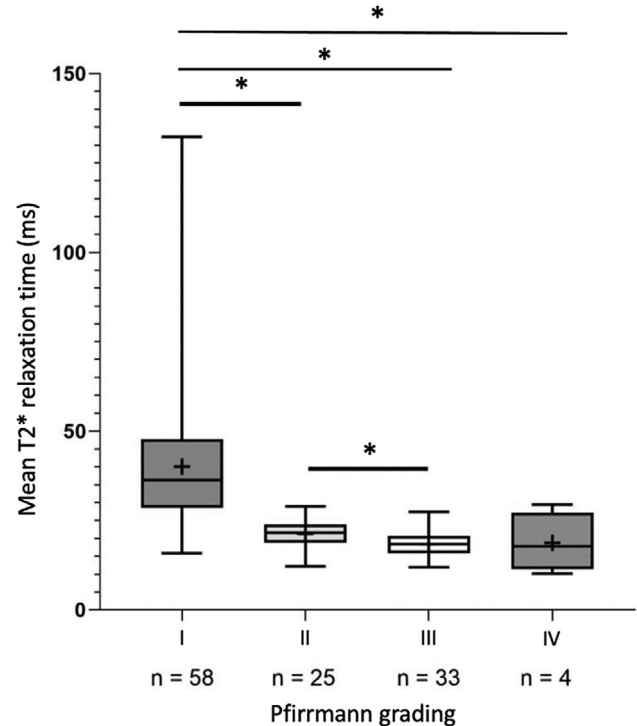


**FIGURE 6** Mean T2\* relaxation time in the nucleus pulposus (NP) of the lumbar canine intervertebral discs (IVD) according to the Pfirrmann grading. The mean T2\* relaxation time of the NP was measured by manually drawing a region of interest (ROI) around the NP of each lumbar canine IVD on the sagittal T2-weighted image and by copying it onto the T2\* mapping image. A negative correlation was found between the T2\* relaxation times and the Pfirrmann grades ( $P < 0.0001$ ). Significant differences were found between grade I and the other grades and between grades II and III ( $*P < 0.05$ ).

three quantitative sequences may provide a more precise overview of the degenerated processes that occur in the IVD. Determination of threshold values would be interesting to more precisely detect and quantify degenerative IVD.

In human medicine, T2 and T2\* relaxation time measurements have been correlated with LBP using different clinical orthopedic pain scores.<sup>13,23</sup> In humans, LBP is mostly due to IVD degeneration, and although it is more difficult to highlight this pain in dogs, it is thought to be similar in veterinary medicine. Indeed, the canine model is one of the only animal models of IVD degeneration to exhibit lumbar or lumbosacral pain with comparable clinical and neurological signs as in human patients suffering from painful IVD.<sup>31</sup> As lumbar or lumbosacral pain was an exclusion criterion in this study, no comparison could be made between nonpainful and painful canine patients. Thus, further investigation would be interesting to apply our quantitative mapping sequences to a cohort of painful dogs. These would aim to assess whether a distinction can be made between healthy and painful IVDs in dogs with lumbar or lumbosacral pain but without disc hernia.

Quantifying the IVD degeneration may be interesting for patient follow-up and longitudinal studies. Irrespective of the treatment chosen, the follow-up could be optimal with a quantified evaluation.



In addition to comparison of the follow-up relaxation times with the previous measurements, the color maps could also be compared with confirm the efficacy of the treatment. Mean values were obtained with the manually-drawn ROI. However, on the color maps, the NP appeared to not be homogeneous. Combining the relaxation time measurements with the color map on which the extreme and aberrant values could be excluded could allow better characterization of the NP degeneration. A pertinent use of these color maps with the exclusion of the aberrant values needs specific software that was not available in our hospital at the time of the study. The measure of the NP relaxation time combined with the results of the corresponding color map will be further assessed to gain sensibility in the characterization of the NP degeneration. Moreover, further longitudinal studies are needed to assess the stability of the relaxation time measurements in healthy canine IVD and to develop these sequences for the evaluation of the efficacy of the chosen treatment.

In conclusion, variable flip angle T1 and multiecho T2 and T2\* relaxation time measurements focused on the NP appear to be repeatable and reproducible. These measurements were shown to be predictive of Pfirrmann IVD grading scores in a small sample of canine patients with no history of lumbar or lumbosacral pain. Complementary to conventional qualitative Pfirrmann grading, these sequences could allow quantification of IVD degeneration. A quantified evaluation of degenerated IVD degeneration could be of interest in the management of painful IVD, especially for the evaluation of the efficacy of regenerative treatments. Further studies are needed to assess the reliability of T1, T2, and T2\* mapping sequences in symptomatic canine patients and longitudinal assessment of canine IVD degeneration.

## LIST OF AUTHOR CONTRIBUTIONS

### Category 1

- (a) Conception and design: Bouhsina, Tur, Hardel, Guicheux, Clouet, Fusellier
- (b) Acquisition of data: Madec, Rouleau, Etienne, Tur, Hardel, Fusellier
- (c) Analysis and interpretation of data: Tur, Fusellier, Bouhsina

### Category 2

- (a) Drafting the Article: Bouhsina, Tur
- (b) Revising article for intellectual content: Madec, Rouleau, Etienne, Hardel, Guicheux, Clouet, Fusellier

### Category 3

- (a) Final approval of the completed article: Bouhsina, Tur, Hardel, Madec, Rouleau, Etienne, Guicheux, Clouet, Fusellier

### Category 4

- (a) Agreement to be accountable for all aspects of the work ensuring that questions related to the accuracy or integrity of any

part of the work are appropriately investigated and resolved: Bouhsina, Tur, Hardel, Madec, Rouleau, Etienne, Guicheux, Clouet, Fusellier

## CONFLICT OF INTEREST STATEMENT

The authors declare no conflicts of interest.

## PREVIOUS PRESENTATION OR PUBLICATION DISCLOSURE

This study was presented at the EVDI Annual Congress, September 11–17, 2022, Edinburgh.

## REPORTING CHECKLIST DISCLOSURE

The ARRIVE guidelines 2.0: author checklist was used for this study.

## DATA ACCESSIBILITY STATEMENT

Readers could access data on request from the the corresponding author.

## ORCID

Nora Bouhsina  <https://orcid.org/0000-0001-7377-4232>

Marion Fusellier  <https://orcid.org/0000-0001-5336-9352>

## REFERENCES

1. Bergknut N, Egenvall A, Hagman R, et al. Incidence of intervertebral disk degeneration-related diseases and associated mortality rates in dogs. *J Am Vet Med Assoc*. 2012; 240:1300-1309.
2. Adams MA, Roughley PJ. What is intervertebral disc degeneration, and what causes it? *Spine (Phila Pa 1976)*. 2006; 31:2151-2161.
3. Whatley BR, Wen X. Intervertebral disc (IVD): structure, degeneration, repair and regeneration. *Mater Sci Eng C*. 2012; 32:61-77.
4. Benneker LM, Heini PF, Anderson SE, Alini M, Ito K. Correlation of radiographic and MRI parameters to morphological and biochemical assessment of intervertebral disc degeneration. *Eur Spine J*. 2005; 14:27-35.
5. Ogon I, Takebayashi T, Takashima H, et al. Imaging diagnosis for intervertebral disc. *Jor Spine*. 2020; 3:1-6.
6. Pfirrmann CWA, Metzdorf A, Zanetti M, Hodler J, Boos N. Magnetic resonance classification of lumbar intervertebral disc degeneration. *Spine (Phila Pa 1976)*. 2001; 26:1873-1878.
7. Kettler A, Wilke HJ. Review of existing grading systems for cervical or lumbar disc and facet joint degeneration. *Eur Spine J*. 2006; 15:705-718.
8. Bergknut N, Auriemma E, Wijsman S, et al. Evaluation of intervertebral disk degeneration in chondrodystrophic and nonchondrodystrophic dogs by use of Pfirrmann grading of images obtained with low-field magnetic resonance imaging. *Am J Vet Res*. 2011; 72:893-898.
9. Welsch GH, Hennig FF, Krinner S, Trattng S. T2 and T2\* Mapping. *Curr Radiol Rep*. 2014; 2:1-9.
10. Welsch GH, Trattng S, Paternostro-Sluga T, et al. Parametric T2 and T2\* mapping techniques to visualize intervertebral disc degeneration in patients with low back pain: initial results on the clinical use of 3.0 Tesla MRI. *Skeletal Radiol*. 2011; 40:543-551.
11. Marinelli NL, Haughton VM, Muñoz A, Anderson PA. T2 relaxation times of intervertebral disc tissue correlated with water content and proteoglycan content. *Spine (Phila Pa 1976)*. 2009; 34:520-524.
12. Takashima H, Takebayashi T, Yoshimoto M, et al. Correlation between T2 relaxation time and intervertebral disc degeneration. *Skeletal Radiol*. 2012; 41:163-167.

13. Ogon I, Takebayashi T, Takashima H, et al. Analysis of chronic low back pain with magnetic resonance imaging T2 mapping of lumbar intervertebral disc. *J Orthop Sci*. 2015; 20:295-301.
14. Chen C, Jia Z, Han Z, et al. Quantitative T2 relaxation time and magnetic transfer ratio predict endplate biochemical content of intervertebral disc degeneration in a canine model. *BMC Musculoskelet Disord*. 2015; 16:1-13.
15. Bouhsina N, Decante C, Hardel JB, et al. Comparison of MRI T1, T2, and T2\* mapping with histology for assessment of intervertebral disc degeneration in an ovine model. *Sci Rep*. 2022; 12:1-12.
16. Ying J, Han Z, Zeng Y, et al. Evaluation of intervertebral disc regeneration with injection of mesenchymal stem cells encapsulated in PEGDA-microcryogel delivery system using quantitative T2 mapping: a study in canines. *Am J Transl Res*. 2019; 11:2028-2041.
17. Ellingson AM, Mehta H, Polly DW, Ellermann J, Nuckley DJ. Disc degeneration assessed by quantitative T2\* (T2 Star) correlated with functional lumbar mechanics. *Spine (Phila Pa 1976)*. 2013; 38:1533-1540.
18. Zhang X, Yang L, Gao F, et al. Comparison of T1 $\rho$  and T2\* relaxation mapping in patients with different grades of disc degeneration at 3T MR. *Med Sci Monit*. 2015; 21:1934-1941.
19. Ellingson AM, Nagel TM, Polly DW, Ellermann J, Nuckley DJ. Quantitative T2\* (T2 star) relaxation times predict site specific proteoglycan content and residual mechanics of the intervertebral disc throughout degeneration. *J Orthop Res*. 2014; 32:1083-1089.
20. Shiguetomi-Medina JM, Gottlieb M, Kristiansen MS, et al. Water-content calculation in growth plate and cartilage using MR T1-mapping design and validation of a new method in a porcine model. *Skeletal Radiol*. 2013; 42:1413-1419.
21. Antoniou J, Pike GB, Steffen T, et al. Quantitative magnetic resonance imaging in the assessment of degenerative disc disease. *Magn Reson Med*. 1998; 40:900-907.
22. Marinelli NL, Haughton VM, Anderson PA. T2 relaxation times correlated with stage of lumbar intervertebral disk degeneration and patient age. *Am J Neuroradiol*. 2010; 31:1278-1282.
23. Blumenkrantz G, Zuo J, Li X, Kornak J, Link TM, Majumdar S. In vivo 3.0-tesla magnetic resonance T 1 $\rho$  and T 2 relaxation mapping in subjects with intervertebral disc degeneration and clinical symptoms. *Magn Reson Med*. 2010; 63:1193-1200.
24. Stelzener D, Welsch GH, Kovács BK, et al. Quantitative T2 evaluation at 3.0 T compared to morphological grading of the lumbar intervertebral disc: a standardized evaluation approach in patients with low back pain. *Eur J Radiol*. 2012; 81:324-330.
25. Antoniou J, Epure LM, Michalek AJ, Grant MP, Iatridis JC, Mwale F. Analysis of quantitative magnetic resonance imaging and biomechanical parameters on human discs with different grades of degeneration. *J Magn Reson Imaging*. 2013; 38:1402-1414.
26. Yoon MA, Hong SJ, Kang CH, Ahn KS, Kim BH. T1 $\rho$  and T2 mapping of lumbar intervertebral disc: correlation with degeneration and morphologic changes in different disc regions. *Magn Reson Imaging*. 2016; 34:932-939.
27. Galley J, Maestretti G, Koch G, Hoogewoud HM. Real T1 relaxation time measurement and diurnal variation analysis of intervertebral discs in a healthy population of 50 volunteers. *Eur J Radiol*. 2017; 87:13-19.
28. Boos N, Wallin A, Schmucker T, Aebi M, Boesch C. Quantitative MR imaging of lumbar intervertebral discs and vertebral bodies: methodology, reproducibility, and preliminary results. *Magn Reson Imaging*. 1994; 12:577-587.
29. Ashinsky BG, Gullbrand SE, Bonnevie ED, et al. Multiscale and multimodal structure-function analysis of intervertebral disc degeneration in a rabbit model. *Osteoarthr Cartil*. 2019; 27:1860-1869.
30. Jazini E, Sharan AD, Morse LJ, et al. Alterations in T 2 relaxation magnetic resonance imaging of the ovine intervertebral disc due to nonenzymatic glycation. *Spine (Phila Pa 1976)*. 2012; 37:209-215.
31. Thompson K, Moore S, Tang S, Wiet M, Purmessur D. The chondrodystrophic dog: a clinically relevant intermediate-sized animal model for the study of intervertebral disc-associated spinal pain. *Jor Spine*. 2018; 1:1-13.

**How to cite this article:** Bouhsina N, Tur L, Hardel J-B, et al. Variable flip angle T1 mapping and multi-echo T2 and T2\* mapping magnetic resonance imaging sequences allow quantitative assessment of canine lumbar disc degeneration. *Vet Radiol Ultrasound*. 2023;64:864-872. <https://doi.org/10.1111/vru.13288>